Probing Molecular Mobility During Crosslinking Process of Commercial Resins by NMR Multiexponential Relaxation Data Analysis

Sérgio de L. Campello,[1] Ricardo E. de Souza,[1,2] Walter M. de Azevedo[1,3]

[1]*Programa de Pós-Graduação em Ciência de Materiais, CCEN, Universidade Federal de Pernambuco, Recife, PE 50670-901, Brazil*
[2]*Departamento de Física, Universidade Federal de Pernambuco, Recife, PE 50670-901, Brazil*
[3]*Departamento de Química Fundamental, Universidade Federal de Pernambuco, Recife, PE 50670-901, Brazil*

Received 14 January 2010; accepted 23 November 2010
DOI 10.1002/app.33827
Published online 16 March 2011 in Wiley Online Library (wileyonlinelibrary.com).

ABSTRACT: In this study, we present the experimental results for the crosslinking process of a commercial polyester resin based on measurements of the spin lattice relaxation time T_1 of protons, as function of the crosslinking time evolution. Multiexponential decomposition of the evolution of magnetization measured in inversion-recovery experiments is performed. The population of "rigid" and "mobile" nuclear spin sites was estimated as function of time evolution. In analogy to the usual monomer conversion u, site conversion from "mobile" to "rigid" sites u_M were also estimated as a function of time evolution and initial concentrations of the reagents. The multiexponential decomposition approach of T_1 relaxation data allows one to follow crosslinking processes. © 2011 Wiley Periodicals, Inc. J Appl Polym Sci 121: 2220–2225, 2011

Key words: crosslinking; kinetics; mobility; relaxation time; NMR

INTRODUCTION

Typically, more than 70% of synthetic polymers for commercial use are crosslinked.[1] Crosslinking density and the mobility of chain segments practically determine mechanical properties of network polymers instead of the chemical structure of network chains.[2] However, information on crosslinking density and the mobility of chain segments are difficult to get by standard chemical techniques. Therefore, several studies of crosslinking polymers by ^{1}H relaxation time measurements[3–5] and NMR imaging[6] were performed, improve knowledge about the mechanism properties. On the other hand, crosslinking kinetics knowledge can be used to improve the design of mechanical properties of polymeric materials. In some cases, crosslinking kinetics could be estimated from imaging experiments.[7] In this case, discrimination can be quite reduced because image intensity values have mixed contributions from both spin–lattice relaxation and spin–spin relaxation processes.[8] Besides, in more complex reticulation processes, the crosslinking agent can be found in different motional regimes. In these cases, it is mandatory to carry out two or more different kinetic studies to rule out any doubt concerning to time evolution of the crosslinking. In the past, spin–lattice relaxation measurements were used to follow curing progress by radical process. However, quantitative conclusions were not straightforward because of the small number of measured points and, as result, they were not very accurate.[9]

In this study, we conducted nondestructive experiments to follow the crosslinking kinetics using nuclear magnetic resonance (NMR) relaxation time measurements and multiexponential relaxation data.[10] The commercial resin crosslinking process and the spatial homogeneity of the reaction were followed by spin–lattice and spin–spin relaxations and MRI measurements as function of reaction time (t_r).

EXPERIMENTAL ASPECTS AND METHOD DESCRIPTION

Material

The commercial resin used in the experiments was the polyester resin, Resapol 10-249, from Reichhold. This material is a high resistant resin used in aggressive atmospheres.[11] The resin cure is induced by addition of the catalyst methyl ethyl ketone peroxide. After the addition of the catalyst, the cure process is fast; however, the cure time can be adjusted as function of the amount of catalyst added to the resin.[12] The polyester resins are unsaturated

Correspondence to: R. E. de Souza (res@df.ufpe.br).

TABLE I
Characteristics of the Resapol 10-249 Resin (Reichhold)

$\overline{M}_n$ (g/mol)	7896
$\overline{M}_w$ (g/mol)	16,442
Acid value (mg KOH/g)	28
Viscosity at 25°C (cP)	1400–1800

polymers of high molecular weight and generally they can be diluted in styrene. Since the styrene molecules are also unsaturated, they can be also responsible for crosslinking the polymer chains.

The resin is based on styrene monomer and polyester containing ethylene glycol and diethylene glycol. Besides there are three acids, maleic, phthalic, and isophthalic. Some characteristics of the resin are summarized in Table I.

The reactions were started by adding the catalyst to resin and stirring the mixture until the solution becomes homogeneous. After that, the solutions were placed in a cylinder sample holder of PVC, which is 5.0 cm high and its internal diameter is 2.5 cm. The sample holder was hermetically closed (oxygen inhibits polymerization process[13–15]) and transferred to the center of rf coil which has an homogeneous region of 7.0 cm in the axial direction. The recommended ratio between the mass of resin m_r and catalyst m_c indicated by the manufacturer is 66.7. The ratio was changed with the purpose of verifying different kinetic regimes of cure. The ratios used in some MRI experiments and spin–lattice relaxation time measurements are indicated in Table II.

TABLE II
Values for m_r/m_c for Various MRI and T_1 Experiments

	MRI			T_1			
Experiment	A	B	C	A	B	C	D
m_r/m_c	60.0	66.7	131.6	33.3	50.0	67.2	133.3

Characterization methods

The NMR experiments were performed on a Varian Inova Unity system operating at 85 MHz ($B = 2.07$ T) for proton resonance. The system operates with a horizontal 30 cm bore size magnet. For a power level of 55 dB, 90° rf pulse length is 36 μs.

Spin echo multi slice sequence (SEMS) were used on MRI experiments. To get T_2 weighted images, echo time T_E and repetition time T_R were adjusted to minimize T_1 effects.[8] This method has been used to follow crosslinking since last decade[16] because T_2 relaxation time is very sensitive to local motions. Thus, the formation of a polymer leads to a change in local motion, as observed by Jackson et al.[7] Since curing process of the Resapol is exothermic, several MRI experiments have been done to verify if there is a possible temperature gradient between central and boundary regions in the sample, resulting in a spatially non homogeneous crosslinking process. Field of view (FOV), image matrix size, and slice thickness of some experiments are indicated in Table III.

Spin–lattice relaxation time T_1 was measured using the inversion-recovery pulse sequence. In nuclear spin systems, where exponential relaxation process prevails with one characteristic mean relaxation time T_1, inversion-recovery sequence provides a z-component magnetization function of inversion time T_i (delay between pulses) given by:

$$M_z(T_i) = M_0[1 - 2exp(-T_i/T_1)] \quad (1)$$

where M_0 is the equilibrium magnetization. In the next section, spin–lattice relaxation time measurements are analyzed considering the spin system response to inversion-recovery pulse sequence.

In addition, spin–spin relaxation time T_2 was measured using CPMG pulse sequence, which provides a transversal component of the magnetization as function of the time delay between pulses τ given by:

$$M_\perp(2\tau) = M_0\exp(-2\tau/T_2) \quad (2)$$

where here we also considered an exponential relaxation process.

It was also measured Young's modulus of the samples used on T_1 experiments. All measurements were carried out using an universal testing machine (EMIC DL-2000) and according to ASTM D638. The Young's modulus was calculated by measuring the slope of stress–strain curve between 0.04% and 0.1% of strain.

RESULTS AND DISCUSSION

Magnetic resonance imaging

Figure 1 presents images of the MRI-A experiment. Under MRI-A experiment conditions (Table III),

TABLE III
MRI Experiment Parameters

Experiment	FOV (mm)	Matrix size ($m \times n$)	Slice thickness (mm)	T_R (ms)	T_E (ms)	Resolution (mm)
MRI-A	30 × 30	64 × 64	10	1500	12.7	0.469 × 0.469
MRI-B	30 × 30	64 × 64	5	1000	12	0.469 × 0.469
MRI-C	50 × 50	128 × 128	5	1000	12	0.391 × 0.391

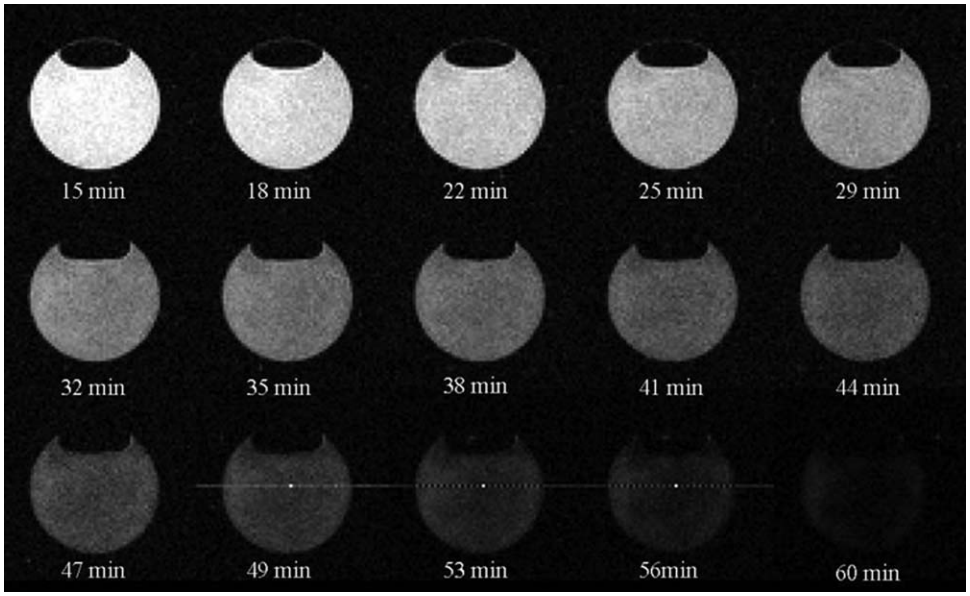

Figure 1 A specific slice images as a function of reaction time (from MRI-A experiment). The dark region on top of images is an air bubble.

imaging intensities are mainly governed by transversal relaxation process. It can be observed from all images that, apparently, intensities of the pixels uniformly decrease in the whole area of the sample as function of reaction time. If relaxation process is dictated by motion regime, it seems that motion picture changes almost at the same rate in the whole sample. To verify this statement, it was performed an intensity image analysis using a software. It was calculated standard deviation σ, considering pixels from a central region on images and from background noise. The results were similar, which indicate that variations of pixel intensity should be smaller than noise level.

Relaxation measurements

All relaxation measurements were made in spectroscopy mode. The T_1 measurements were performed along with curing process of resin. All repetition times in relaxation measurements were adjusted to 2.5 s because T_1 value in liquid resin without catalyst is 520 ms. However for long reaction times, fitting process using eq. (1) is quite inadequate. To illustrate this aspect, Figure 2(a,b) indicate the fitting curve and the corresponding experimental data at two different reaction times. The relaxation function in Figure 2(a) was measured at reaction time $t_r = 19$ min. The continuous line is the fitting function using eq. (1). Figure 2(b) indicates the best fitting curve and relaxation function at reaction time $t_r = 130$ min.

These results suggest that the previously commented assumption that there is just one exponential process, with mean value relaxation time T_1 [eq. (1)], is not appropriate to describe the relaxation process for long reaction times.

To describe this regime more accurately, it was adopted that molecular motion around A-type nuclear spins regions is quite distinct of B-type ones. This means that relaxation process of the j-type site (with j = A, B, etc.) is exponential with characteristic relaxation time T_{1j}. Besides, apparently, there is no significant magnetization diffusion between sites; otherwise relaxation times would be similar. Considering A and B sites only, inversion-recovery experiments should produce signals as:

$$M_z(T_i) = M_{0A}[1 - 2\exp(-T_i/T_{1A})] + M_{0B}[1 - 2\exp(-T_i/T_{1B})] \quad (3)$$

where M_{0A} and M_{0B} are equilibrium magnetizations of A and B regions and T_{1A} and T_{1B} are characteristic relaxation times of A and B regions, respectively. Thus, M_{0A} and M_{0B} are proportional to spin density in these sites. This approach was used by Geppi et al.[17] to probe molecular motions of polymeric materials above the glass transition temperature. However, in that study, the multiexponential behavior was observed by spin–lattice relaxation time in the rotating frame $T_{1\rho}$. The results indicate differences in T_{1A} and T_{1B} by a factor of two orders of magnitude and M_{0A} and M_{0B} varying as a function of reaction time. The larger value of T_1 (T_{1M}) was associated with the most mobile site, that will be represented by $[M](t_r)$, while smaller T_1 value (T_{lR}) will be associated with the most rigid site, that will be represented by $[R](t_r)$. According to Currie Law, the values of $[M](t_r)$ and $[R](t_r)$ are proportional to spin

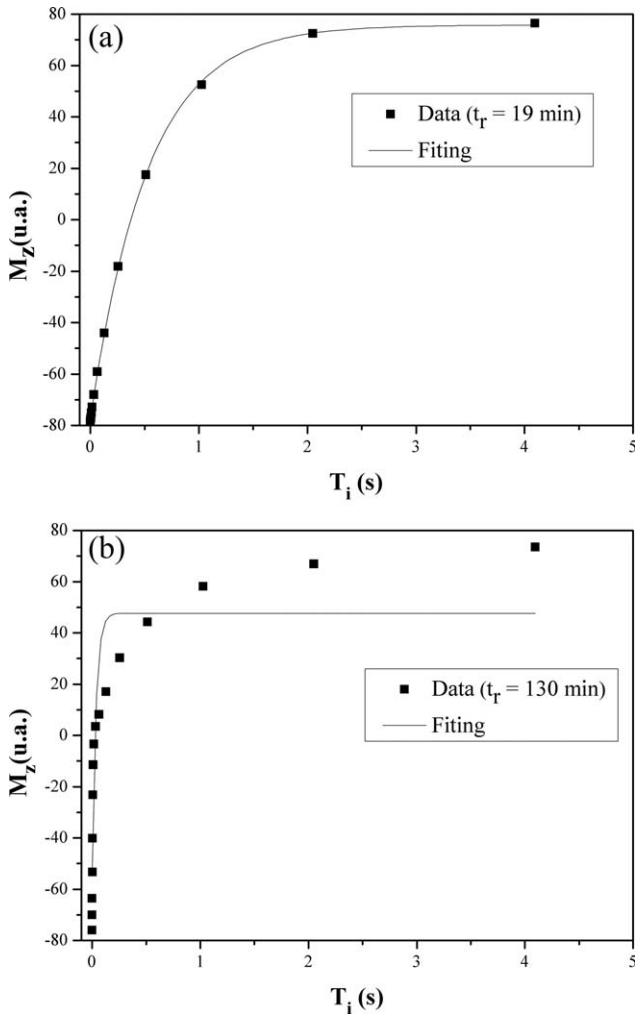

Figure 2 (a) Experimental data and fitting curve using eq. (1) for $t_r = 19$ min.; (b) Experimental data and fitting curve using eq. (1) for $t_r = 130$ min.

densities of mobile and rigid sites and also to the concentration of these sites, respectively.

In the model, it was adopted that there are only two kinds of sites present in the system. Equations (4) and (5) are normalized $[M](t_r)$ and $[R](t_r)$:

$$[M](t_r) = \frac{M_{0A}(t_r)}{M_{0A}(t_r) + M_{0B}(t_r)} \quad (4)$$

$$[R](t_r) = \frac{M_{0B}(t_r)}{M_{0A}(t_r) + M_{0B}(t_r)} \quad (5)$$

The results obtained for these populations in experiments T1-A and T1-C are shown in Figure 3(a,b), respectively.

At the beginning, for small reaction times, the concentration of mobile sites is high while the concentration of rigid sites is almost null. It explains the successful fitting using one exponential [eq. (1)] of the relaxation data for small times [Fig. 2(a)]. After induction time, the concentration of mobile sites rapidly decreases causing an increase on concentration of rigid sites. The gel effect can be observed starting from $t_r = 20$ min for T1-A and $t_r = 46$ min for T1-C experiment, while glass effect can be considered starting from $t_r = 60$ min for T1-A and $t_r = 150$ min for T1-C. At the end of experiment, the concentration is 43% for mobile sites and 57% for rigid sites for T1-A. In the experiment T1-C, the final concentrations of mobile and rigid sites are 47 and 53%, respectively. Each experiment is ended when there is no significant change in T_1 values.

The mobile site conversion u_M into rigid site can be defined as:

$$u_M(t_r) = 1 - \frac{[M](t_r)}{[M](0)} \quad (6)$$

The analysis of the mobile site conversion can help the selection of cure parameters as reaction time and final conversion. Figure 4(a) illustrates the

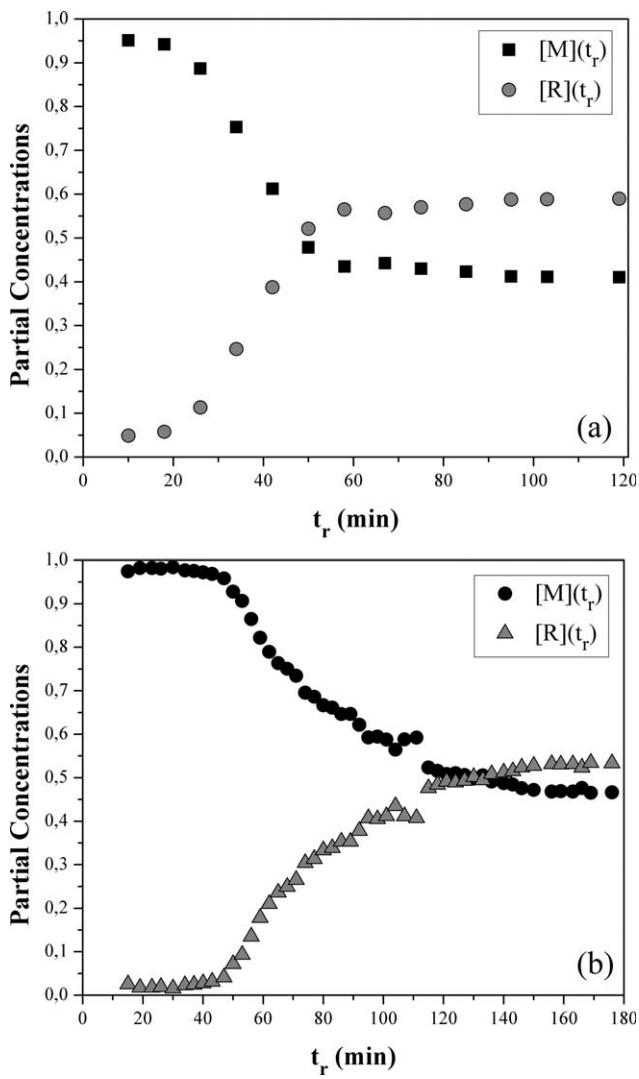

Figure 3 (a) Concentrations of mobile and rigid sites obtained in experiment T1-A. (b) Concentrations of mobile and rigid sites obtained in experiment T1-C.

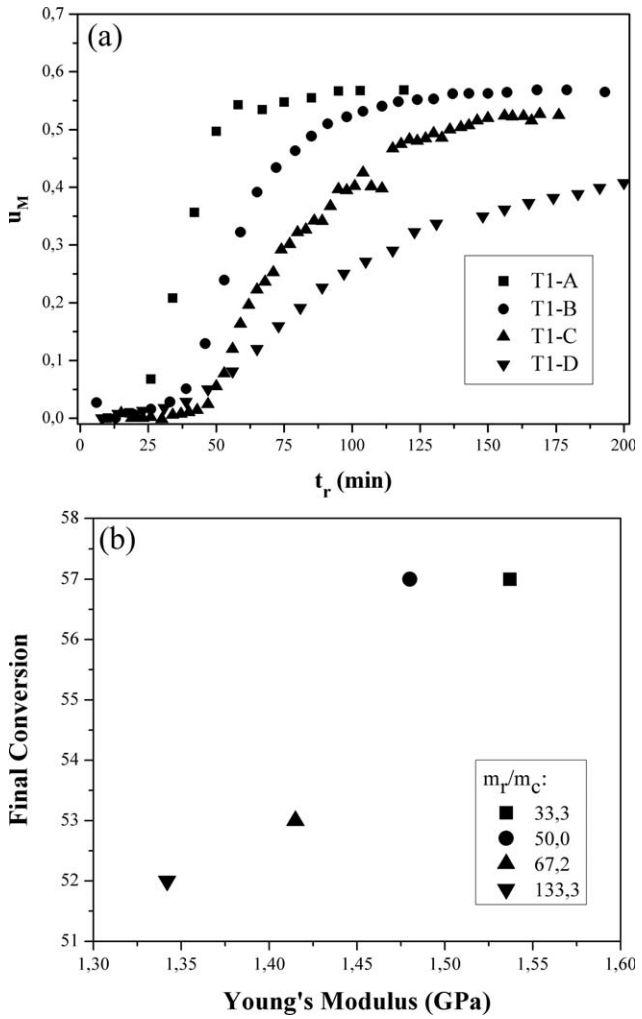

Figure 4 (a) Mobile site conversion as a function of time for different ratios m_r/m_c listed in Table II. (b) Final mobile site conversion, obtained by NMR, versus Young's modulus, for different m_r/m_c ratios.

mobile site conversion of four different experiments, which proportions of resin and catalyst are indicated in Table II. The reaction time, the velocity of reaction, and the final mobile site conversion can be adjusted by the increase of catalyst concentration. From these results, the most pronounced change can be seen in the T1-A experiment.

Figure 4(a) also clearly shows that an increasing catalyst concentration results in a reaction velocity enhancement, as expected, as well as the final mobile sites conversion. Consequently, the interval of time that reaction remains on gel regime is reduced. The period of gel regime for T1-A experiment is about 40 min while for T1-C it is around 100 min. Both final mobile site conversions for the T1-A and T1-B experiments are 57%, while for T1-C and T1-D, they are 53 and 52% [at $t_r = 440$ min, in Fig. 4(a) this instant time is out of range], respectively. Although in most experiments a little more than 50% of the mobile sites have been converted, all samples present high mechanical rigidity at the end of reaction process.

To correlate mechanical rigidity with final conversion, it was carried out Young's modulus measurements as a function of the ratio m_r/m_c. The results are shown in Figure 4(b) where it can be noted that the final conversion, obtained by NMR, is increasing with the Young's modulus. There is some correlation between Young's modulus and final conversion; however, a high Young's modulus value does not mean a high final conversion. It looks that Young's modulus value is also determined by the specific kinetics of the reaction. It should be remarked that the most suitable ratio, recommended by the manufacturer, was used in the T1-C experiment. According to these results, we may conclude that there are others ratios that can be a better choice, since they can result in larger final mobile site conversions in shorter times and larger mechanical rigidity.

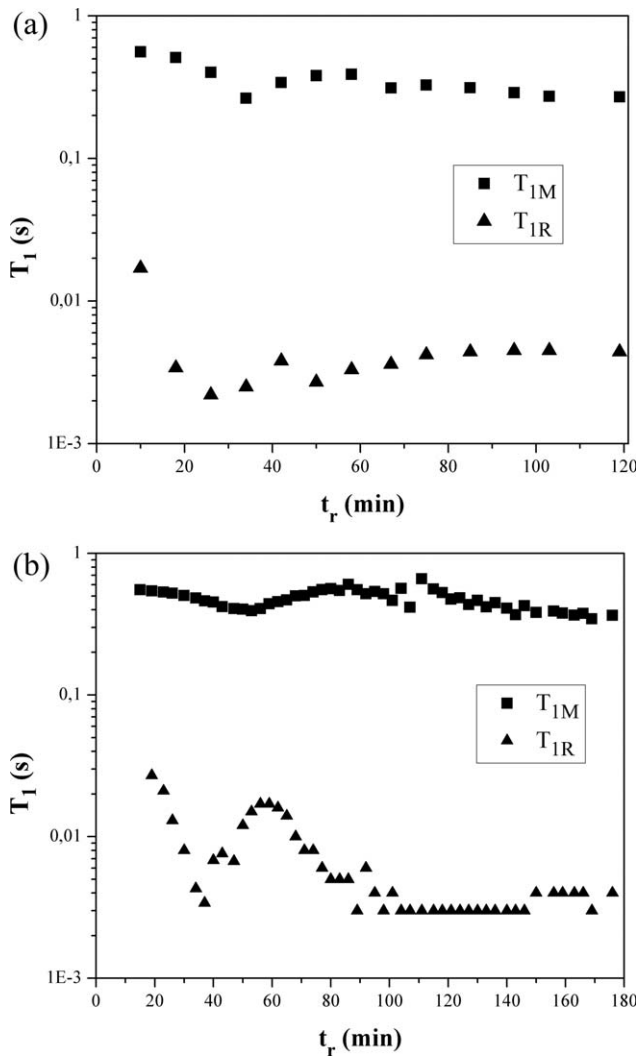

Figure 5 (a) T_{1M} and T_{1R} obtained from the fitting using eq. (3) for T1-A experiment. (b) T_{1M} and T_{1R} obtained from the fitting using eq. (3) for T1-C experiment.

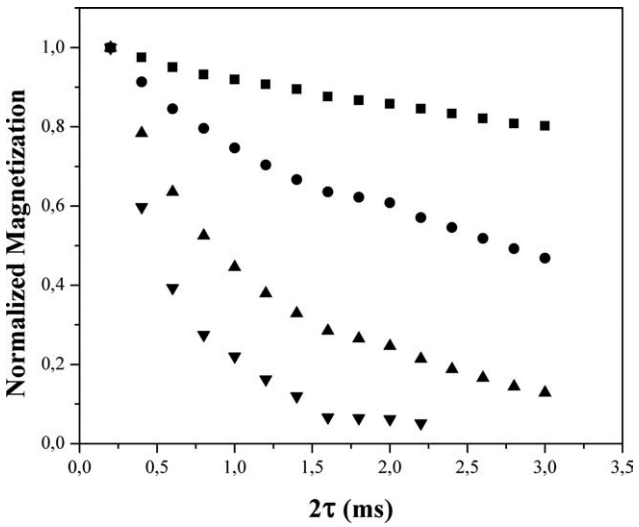

Figure 6 Transversal magnetization (normalized) versus echo time. T_2 values obtained from the fitting using eq. (2) for different reaction times: (■) T_2 (t_r = 46 min) = 13 ms; (●) T_2 (t_r = 72 min) = 3.8 ms; (▲) T_2 (t_r = 104 min) = 1.2 ms; and (▼) T_2 (t_r = 162 min) = 0.50 ms.

Figure 5 shows T_1 measurements as a function of reaction time. The values of T_{1M} and T_{1R} were obtained from the biexponential fitting function [eq. (3)] for T1-A and T1-C experiments. There can be observed differences around two orders of magnitude of T_{1M} and T_{1R} values in each experiment. T_1 differences, during reaction, indicate quite distinct motion regimes for mobile and rigid sites. Both T_{1M} and T_{1R} measurements present double-wing-shape curves, despite T_{1R} curve is more pronounced. This discrepancy indicates that rigid sites experience a significant change in neighborhood motion regime during curing process which is in accord with a picture of the crosslinking formation. Although Paci et al.[9] has also observed an initial biexponential behavior, it disappears as the reaction proceeds. In that work,[9] the T_1 values of the rigid and mobile sites tend to be equal. The shapes of the curves are similar to that one found in the mentioned work.

Usually ^1H spin–spin relaxation time T_2 is a more sensitive and specific parameter concerning to changing molecular motion, as it can be seen in the NMR literature.[1,5,6] However, for this system, T_2 measurements under several conditions have showed that magnetization decay is always monoexponential. Figure 6 shows some magnetization decay measurements during reaction time for a sample prepared following ratio m_r/m_c recommended by the manufacturer. All curves can be fitted by a monoexponential decay characterizing a single T_2 value. T_2 measurements cannot be used to discriminate rigid sites from mobile sites in this system.

CONCLUSIONS

The analysis of measurements based on the multiexponential decomposition of T_1 relaxation data allows to follow crosslinking processes. This procedure enables one to follow the site concentration during the curing process. Mobile site conversions obtained by this procedure clearly show induction, gel and glass phases. Parameters such as induction time, gel phase time, and reaction velocity can be extracted from site conversion curves. The procedure is also appropriate to study motion regimes by T_1 values during crosslinking process. It has been applied to follow the cure kinetics in polyester-based resins prepared under different conditions. Although the procedure should be compared to other methods, it is expected that it complements studies on polymerization kinetics.

Sérgio de L. Campello thanks CAPES for Ph.D grant and professor A. Galembeck for the helpful discussions. We also thank Mr. R. Gomes, from Escola Técnica SENAI Santo Amaro–Manoel de Brito, for assistance with the elastic modulus measurements and Ms. M. Costa for the grammar review.

References

1. Andreis, M.; Koenig, J. L. Adv Polym Sci 1989, 89, 69.
2. Elias, H. G. An Introduction to Polymer Science; VCH Publishers: Weinheim, 1997; Chapter 2.
3. Rowland, T. J.; Labun, L. C. Macromolecules 1978, 11, 466.
4. Douglass, D. C.; McBrierty, V. J. J Chem Phys 1971, 54, 4085.
5. Andreis, M.; Veksli, Z.; Ranogajec, F.; Hedvig, P. Polymer 1989, 30, 1498.
6. Kuhn, W.; Barth, P.; Hafner, S.; Simon, G.; Schneider, H. Macromolecules 1994, 27, 5773.
7. Jackson, P.; Clayden, N. J.; Walton, N. J.; Carpenter, T. A.; Hall, L. D.; Jezzard, P. Polym Int 1991, 24, 139.
8. Haacke, E. M.; Brown, R. W.; Thompson, M. R.; Venkatesan, R. Magnetic Resonance Imaging: Physical Principles and Sequence Design; Wiley: New York, 1999; Chapter 15.
9. Paci, M.; Dei Vecchio, E.; Campana, F. Polym Bull 1986, 15, 21.
10. Kleinberg, R. L.; Kenyon, W. E.; Mitra, P. P. J Magn Reson A 1994, 108, 206.
11. Curing Data Sheet Dion 9100, Reichhold (2004). Available at http://www.reichhold.com/pt/composites-brochures.aspx.
12. Hsu, C. P.; Lee, L. J. Polymer 1993, 34, 4496.
13. Guillot, G.; Nunes, T. G.; Ruaud, J. P.; Polido, M. Polymer 2004, 45, 5525.
14. Decker, C.; Jenkins, A. D. Macromolecules 1985, 18, 1241.
15. Rueggeberg, F. A.; Margeson, D. H. J Dent Res 1990, 69, 1652.
16. Balcom, B. J.; Carpenter, T. A.; Hall, L. D. Macromolecules 1992, 25, 6818.
17. Geppi, M.; Harris, R. K.; Kenwright, A. M.; Say, B. J Solid State Nuclear Magn Reson 1998, 12, 15.